JOURNAL OF MATERIALS SCIENCE 30 (1995) 1584–1594

Strontium modification of aluminium alloy castings in the expendable pattern casting process

L. WANG, S. SHIVKUMAR*
Department of Mechanical Engineering, Worcester Polytechnic Institute, Worcester, MA 01609, USA

The influence of strontium modification on microstructure, pore characteristics and tensile properties of Al–Si–Cu castings produced by the expendable pattern casting (EPC) process has been investigated. Test castings have been produced at strontium concentrations varying from 0.0004%–0.03%. The castings have been analysed by microscopic and image analysis techniques. The results indicate that optimum strontium concentrations are between 0.01% and 0.015%. A coarsening of silicon particles is observed at strontium concentrations greater than 0.015%–0.02%. The addition of strontium to the melt also refines the iron- and copper-bearing phases in the casting. The amount of bulk porosity, average pore size and tensile properties of modified EPC castings are comparable to green sand castings. EPC castings are prone to surface porosity. Strontium modification has a significant effect on the pore distributions in EPC castings. The overall porosity and the maximum pore size increase with strontium modification.

1. Introduction

The expendable pattern casting (EPC) process utilizes foamed polymer prototypes for the production of the cast component. The desired shape is initially replicated in the polymer (typically expanded polystyrene (EPS)) through injection moulding techniques. The polymer pattern is then coated with a ceramic slurry and buried in loose sand. The sand is thoroughly compacted and molten metal is poured directly on to the polymer pattern. The polymer undergoes thermal degradation through a series of transitions and is gradually replaced by the molten metal to yield the casting after solidification. The EPC process has emerged as a viable alternative to conventional empty-cavity casting methods for the fabrication of near-net shape components. Numerous technological reviews in the published literature summarize the operating principles and the advantages of this casting technique [1–6]. The physico-chemical mechanisms associated with the formation of the casting and aspects related to the metallurgical quality of the cast component have been described in recent publications [7–11].

Al–Si–Cu alloys belonging to the 319 family of casting alloys are often used with the EPC process. The morphology of the eutectic silicon in these alloys may have a strong influence on mechanical properties of the casting. The silicon particle morphology can be controlled by adjusting the cooling rate or, more commonly, by the addition of strontium-containing master alloys to the melt. The addition of strontium results in a fine and fibrous silicon structure during solidification and produces several benefits. The beneficial effects of strontium modification in aluminium castings produced by conventional empty-cavity processes have been well documented [12, 13]. It has been shown that strontium modification may improve ductility, fracture, fatigue and impact properties. Furthermore, strontium modification can effectively be used to reduce the solution treatment times in the T6 temper [14]. Despite these benefits, however, there is a degree of apprehension associated with modification, primarily because of the apparent increase of porosity in the casting.

In the present contribution, the results of a fundamental study on the quality of strontium-modified aluminium castings produced by the EPC process are presented. Although the EPC process is being used to produce a wide variety of commercial castings, there is a dearth of information pertaining to the quality of the cast component. This study is aimed at evaluating the effects of strontium modification on microstructure and porosity.

2. Experimental procedure

The patterns and their gating systems (Fig. 1) were prepared by means of a hot-wire cutter from solid

* Author to whom all correspondence should be addressed.

0022–2461

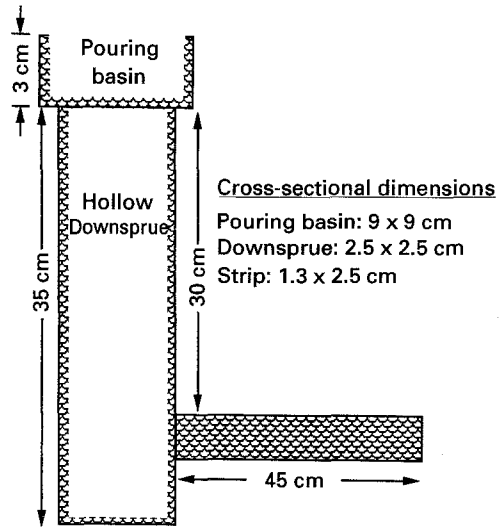

Figure 1 Schematic illustration of the test pattern used in the experiments.

TABLE I Chemical composition of the alloy

Element	(%)
Si	5.90
Cu	3.23
Zn	0.75
Fe	0.93
Mn	0.34
Mg	0.06
Ti	0.05
Cr	0.06
Ni	0.03
Sr	0.00
Al	Balance

expanded polystyrene blocks and plates with a nominal density 0.02 g cm^{-3} and a bead size of about 2 mm (T beads) [7]. The patterns were coated by dipping in a commercial refractory slurry (Styrokote 145.3 PM) of fixed density (43 Baumé). The coated pattern was dried overnight at a temperature of 45 °C in a circulating hot-air stream. The prepared pattern was placed in a steel box and filled with unbonded sand with an AFS grain size number of 55. The steel box was vibrated periodically to compact the sand. A ceramic pouring basin was then positioned on the pattern and secured tightly to avoid displacement during pouring.

The metal, consisting of 100% alloy 319, was melted in a clay graphite crucible using a high-frequency (10 kHz) induction furnace. The chemical composition of the alloy used in all the experiments is shown in Table I. The temperature of the metal was increased to 650 °C. A stainless steel tube with circumferential holes of diameter 1.5 mm was then inserted into the melt of degas the metal. The melt was degassed with high-purity (99.999%) nitrogen for at least 60 min. Vacuum degassing samples were cast periodically to check the gas content of the melt. Degassing was continued during the entire duration of the experiment. Two castings were produced in the unmodified condition, i.e. before the addition of the modifier.

TABLE II Average grain size and secondary dendrite arm spacing (DAS) in the casting as a function of the distance from the downsprue (strontium content = 0.011%)

	Distance from downsprue (cm)				
	1	7.5	22.5	37.5	44
Grain size (μm)	2910	2540	1600	440	320
Dendrite arm spacing (μm)	40.0	36.1	31.9	28.7	24.7

Subsequently, modified castings were produced by adding appropriate amounts of Al–9.7% Sr master alloy to the melt. Predetermined amounts of the master alloy were periodically added to the melt to produce castings at strontium concentrations ranging from about 0.005%–0.03%. Thus, castings containing various amounts of strontium were produced from the same melt. The pouring temperature for all castings was maintained at 750 ± 5 °C. Several sand and permanent mould strip castings were also produced from modified melts. Sand castings were produced in green sand moulds while permanent mould castings were poured into cast iron moulds at room temperature.

The cast strips were analysed by metallographic techniques. Each strip was sectioned at several locations and examined by optical and scanning electron microscopy to determine the variation in microstructure as a function of the distance from the downsprue. The dendrite arm spacing was determined in all the sections. Various phases in the microstructure were identified in terms of composition and morphology. The Kevex image analysis system was used to characterize the distribution and morphology of silicon particles. A minimum of 15 (and up to 30) fields were analysed for each specimen. Density measurements were conducted to determine the extent of porosity in the casting. Image analysis techniques were also used to quantify the amount of porosity. Tensile specimens (ASTM E8) were machined from the cast strip to determine yield strength (0.2% proof strength), ultimate tensile strength and per cent elongation. At least two tests were conducted under identical conditions.

3. Results

The thermal degradation of polystyrene is a highly endothermic process and requires energies in excess of 1200 J g^{-1} of EPS [15]. Hence, during the filling of the mould, steep thermal gradients are established in the casting. These gradients ensure directional solidification of the casting and the local solidification time, θ, is a function of the location in the casting. The respective values of θ have been measured to be of the order of 175 and 100 s at distances of 1 and 40 cm from the downsprue. Because of this variation in θ, the equiaxed dendritic structure in the casting is progressively refined along the length of flow. Average values of grain size and secondary dendrite arm spacing (DAS) at several locations in the test casting are presented in Table II. Strontium modification did not have any significant effect on grain size or DAS.

TABLE III Variation of average Si particle size (D) and aspect ratio (AR) as a function of Sr concentration and distance from the downsprue

Sr content (wt %)	Distance from the downsprue					
	1 cm		22.5 cm		44 cm	
	D (μm)	AR	D (μm)	AR	D (μm)	AR
0.0004	3.97	2.58	3.70	2.57	3.25	2.50
0.0043	2.93	2.36	2.52	2.31	1.97	2.10
0.0076	1.86	1.87	1.75	1.95	1.62	1.86
0.0108	1.76	1.86	1.86	1.88	1.72	1.84
0.0152	1.84	1.86	2.06	1.87	1.74	1.78
0.0255	1.82	1.93	1.95	1.86	1.68	1.80

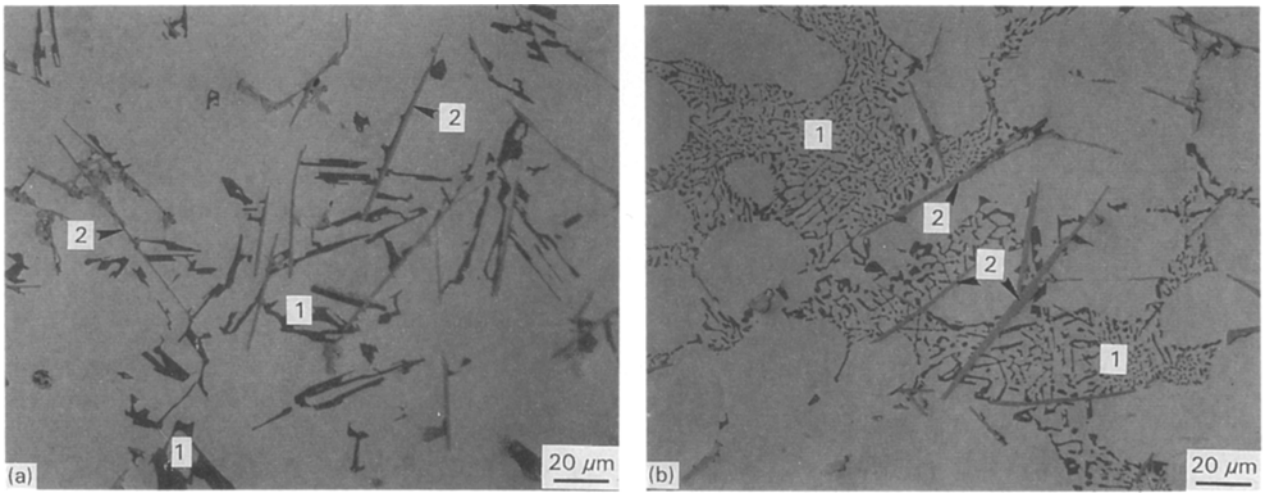

Figure 2 Photomicrographs showing the Si (1) structure in (a) unmodified and (b) strontium-modified alloys. The morphology of $FeSiAl_5$ (2) phase is also shown. The strontium content in the modified alloy is measured to be 0.011%.

Because alloy 319 contains several alloying elements, a variety of interdendritic phases can be detected in the casting. These phases include silicon, $(Fe, Mn)_3Si_2Al_{15}$, $FeSiAl_5$, Al_2Cu and $Al_5Mg_8Cu_2Si_6$. The distribution and morphology of these phases are influenced by location in the casting (or local solidification time) and by strontium modification. For example, in unmodified alloys, the average size of silicon particles is measured to be of the order of 4 μm at a distance of 1 cm from the downsprue (Table III). By comparison, the average silicon particle size is 3.2 μm at a distance of 44 cm. Thus, there is a progressive refinement of silicon particles along the length of flow. The effect of strontium modification on silicon particle morphology is shown in Fig. 2. It is clear that the addition of strontium refines the silicon particles. Deep-etched photographs shown in Fig. 3 highlight the effect of strontium concentration on silicon particle morphology. At strontium concentrations less than 0.005%, the faceted silicon phase grows primarily as plates or needles. With increasing strontium addition, silicon particles are broken down into smaller fragments and a fibrous structure is observed at concentrations of 0.01%–0.015%. Increasing the strontium content beyond about 0.015% may lead to "overmodification" and results in a slight coarsening of silicon particles (Fig. 3d). It should be noted that this coarsening does not occur uniformly throughout the sample. Isolated areas of overmodification are usually present together with a well-modified eutectic silicon structure. Image analysis data on silicon particle morphology are presented in Table III. The average equivalent diameter of silicon particles decreases from about 4 μm in unmodified alloys to about 1.8 μm at strontium concentrations of 0.01%. The image analysis data also indicate a coarsening of silicon particles at strontium contents greater than 0.010%–0.015% for all three solidification times shown in Table III.

Alloy 319 may contain two principal iron-bearing phases: $(Fe, Mn)_3Si_2Al_{15}$ and $FeSiAl_5$. The local cooling rate and strontium modification may have a significant effect on the amount and size of these phases, as shown in Fig. 4. At locations near the downsprue, large $(Fe, Mn)_3Si_2Al_{15}$ Chinese script particles can be observed (Fig. 4a). As the distance from the downsprue increases, the Chinese script particles become smaller, increase in number and are distributed more uniformly. Strontium modification lowers the size of the script particle significantly (Fig. 4d). Typical size of the Chinese script particle has been measured to be of the order of 110 and 65 μm in unmodified and

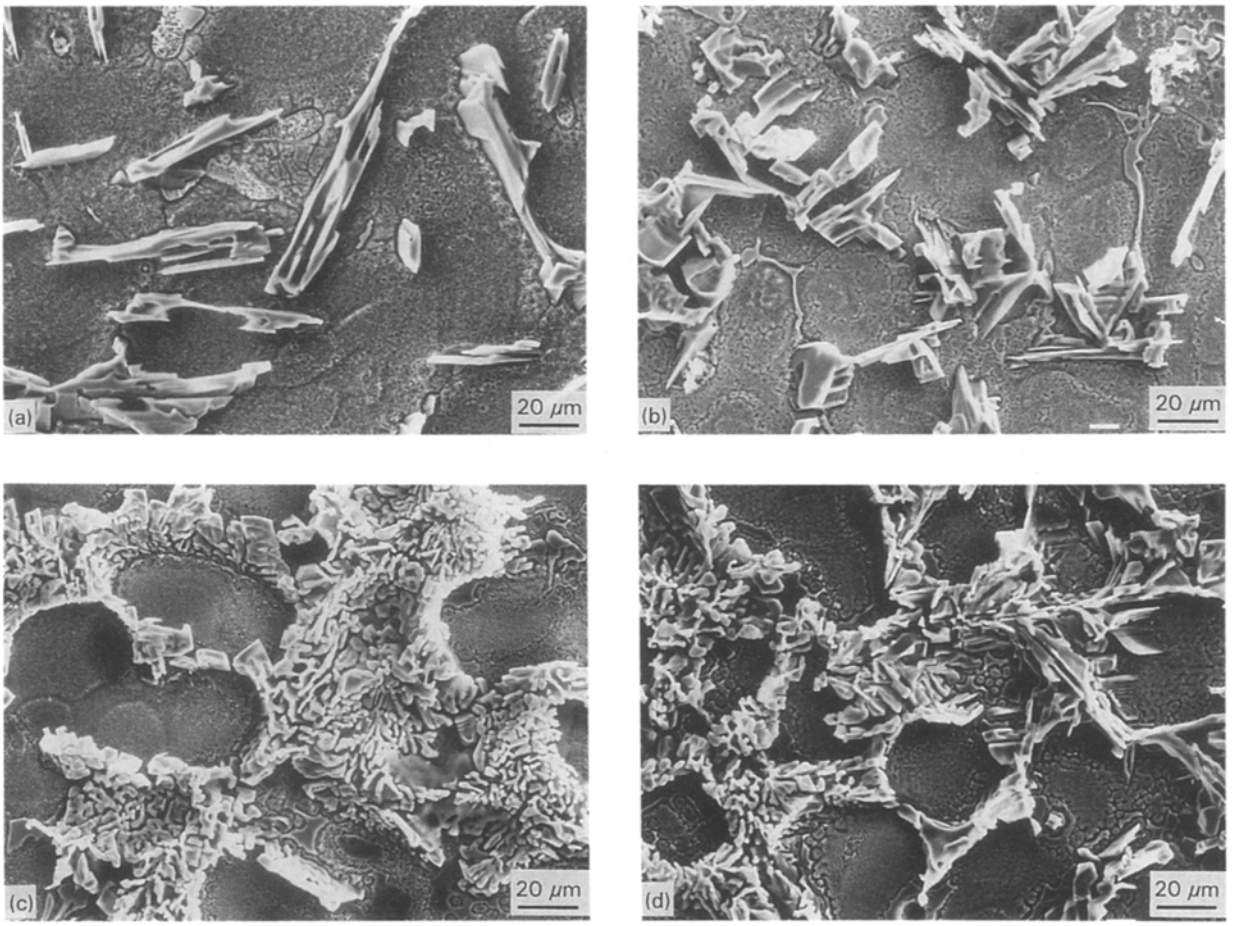

Figure 3 Deep-etched photomicrographs showing the silicon particle morphology as a function of strontium content (distance from downsprue = 22.5 cm). (a) 0.0004%, (b) 0.011%, (c) 0.15%, (d) 0.025%.

strontium modified (strontium content = 0.01%) castings. The $FeSiAl_5$ phase is not detected up to about 30 cm from the downsprue. At distances greater than 30 cm, $FeSiAl_5$ needles are clearly observed in the microstructure (Fig. 2). The aspect ratio of the needles varies from about 4–65. Strontium modification does not have any significant effect on the distribution or morphology of the iron needles.

The copper-bearing phases form towards the end of solidification and consequently may be nucleated on other interdendritic particles (Fig. 5a). Two types of copper phase are detected: Al_2Cu and $Al_5Mg_8Cu_2Si_6$. In unmodified alloys, copper is present primarily as Al_2Cu (Fig. 5a) at locations near the downsprue. As the distance from the downsprue increases, the size of the Al_2Cu phase decreases and at distances greater than about 30 cm, large amounts of $Al_5Mg_8Cu_2Si_6$ begin to form (Fig. 5c). In modified alloys, nearly all the copper is present in the form of $Al_5Mg_8Cu_2Si_6$ (Fig. 5d–f). The average size of the copper phase decreases upon strontium modification.

The variation of porosity in unmodified and strontium-modified (0.015% Sr) casting with the location in the casting is shown in Fig. 6. The amount of porosity generally decreases with distance from the downsprue. Unmodified castings contain a relatively large number of small isolated pores. The amount of porosity and average pore size increases upon modification. Most of the porosity in modified alloys follows the grain boundaries. In unmodified alloys, the large pores are along the grain boundaries while many small pores are confined to the interdendritic regions. Pore distributions plotted in Fig. 7 indicate that at low strontium concentrations (0.0004%), the distribution is skewed towards small pores. As the strontium concentration is increased, the pore distribution gradually becomes skewed towards larger pores. Image analysis data on pore characteristics at a distance of 22.5 cm from the downsprue are shown in Table IV. It is generally observed that the pore size increases with the addition of strontium and the pore density decreases.

The pores observed in unmodified and modified samples were classified based on the degree of circularity. A circularity shape factor (CSF), defined as the ratio of the perimeter of a circle that has the same area as the feature to the feature's perimeter, was used for the classification. It was generally observed that pores with CSF less than about 0.75 were highly irregular and branched, while pores with CSF greater than 0.85 were quite spherical (Fig. 8). Pores with CSF between 0.75 and 0.85 exhibited intermediate shapes (Fig. 8b). The classification was conducted based on number and area as shown in Table V. Classification based on number was conducted by determining the ratio between the *number* of pores with CSF less than the

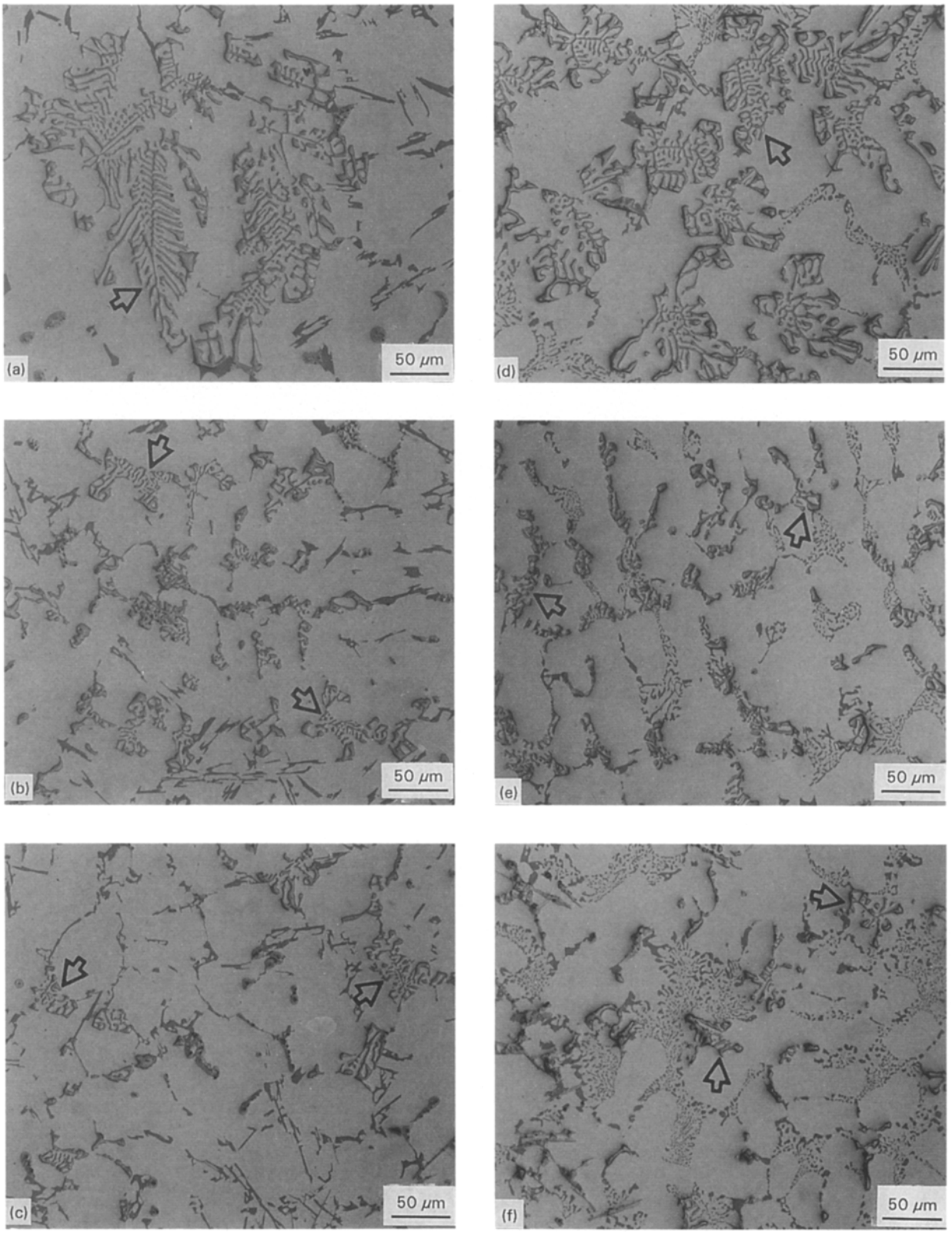

Figure 4 Photomicrographs showing the distribution and morphology of $(Fe,Mn)_3Si_2Al_{15}$ Chinese script particles as a function of the distance from the downsprue. The arrows indicate the Chinese script particles. Unmodified: (a) 1 cm, (b) 22.5 cm, (c) 44 cm. Strontium-modified (strontium content = 0.011%): (d) 1 cm, (e) 22.5 cm, (f) 44 cm.

desired value to the *total number* of pores in the casting. In order to conduct the classification based on area, the number of pores below the desired value of CSF was determined and the area occupied by these pores was calculated. The ratio between this *area* and the *total area* of all the pores in the casting is presented in Table V. It can be seen that the number of highly irregular pores decreases slightly upon modification. The number of intermediate pores does not change significantly. The number of circular pores increases

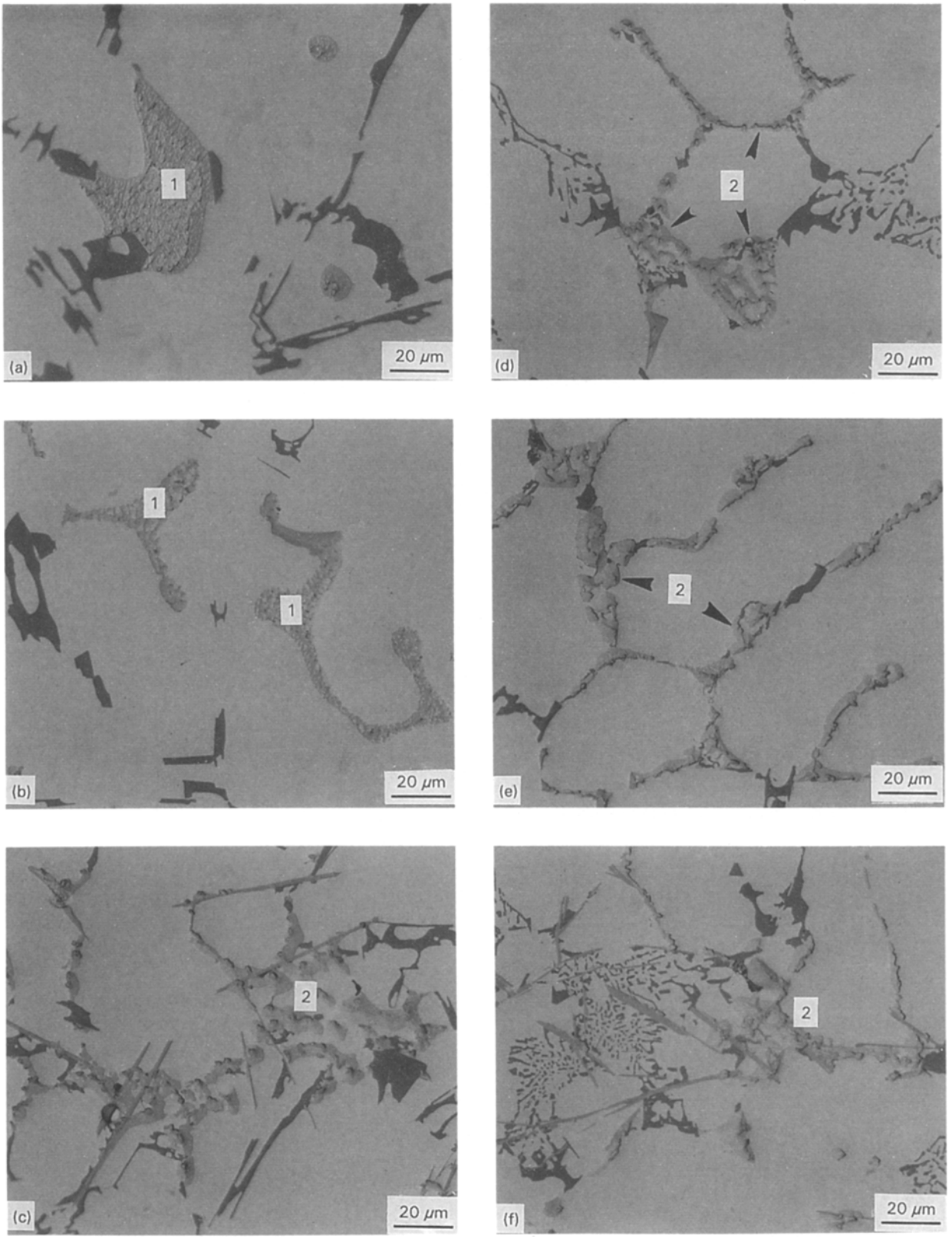

Figure 5 Photomicrographs showing the distribution and morphology of copper-bearing phases as a function of distance from downsprue: (1) Al_2Cu and (2) $Al_5Mg_8Cu_2Si_6$. Unmodified: (a) 1 cm, (b) 22.5 cm, (c) 44 cm. Strontium-modified (strontium content = 0.011%): (d) 1 cm, (e) 22.5 cm, (f) 44 cm.

with the addition of strontium to the melt. For example, the fraction of pores with CSF greater than 0.85 increases from about 20.3% to 36% upon the addition of 0.01% Sr. Note also that the area occupied by pores with CSF greater than 0.85 increases with strontium concentration indicating that large, nearly spherical pores contribute substantially to the overall pore area in modified samples.

Because solidification occurs under steep thermal gradients, the distribution of porosity may vary with

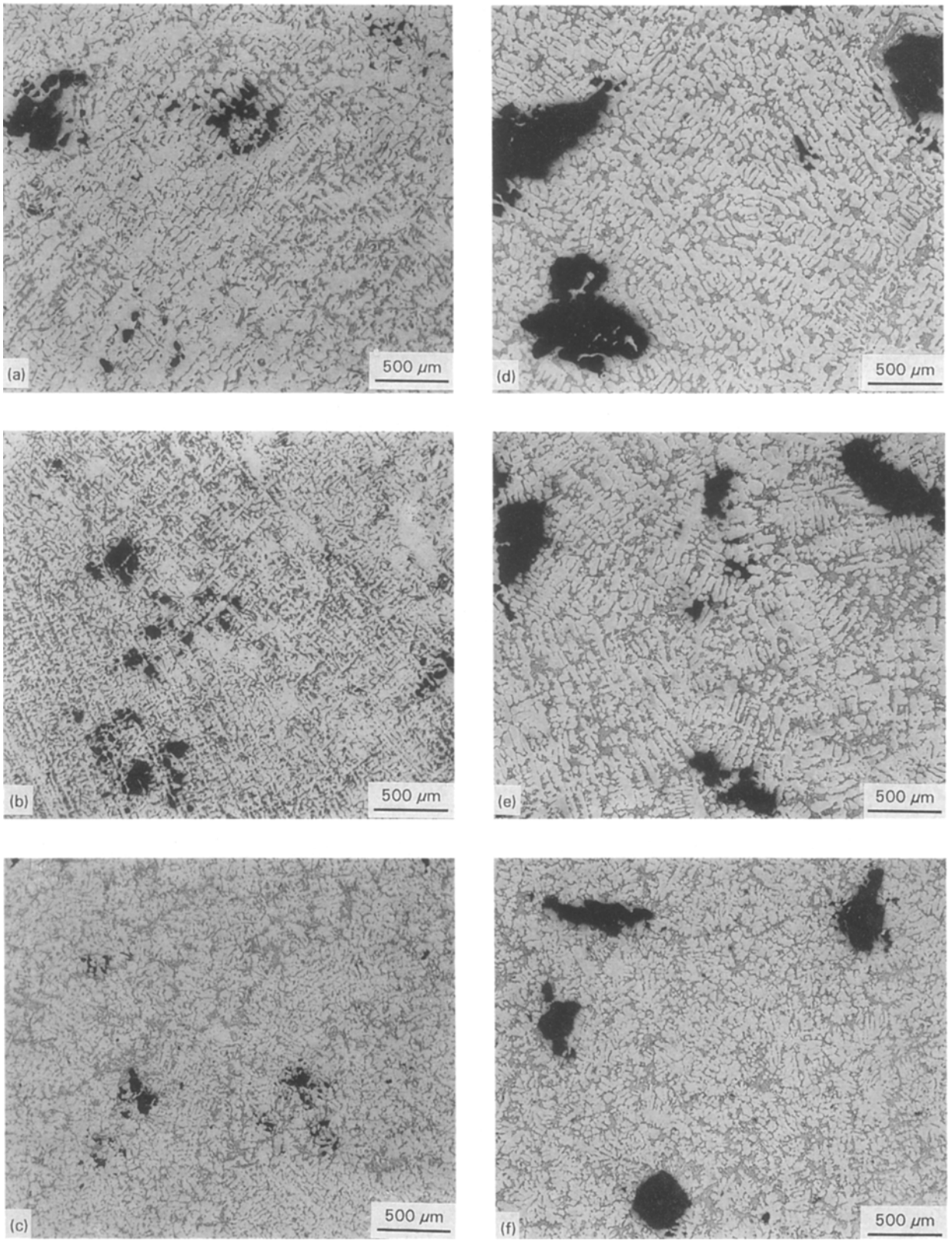

Figure 6 Photomicrographs showing porosity distribution in test castings as a function of distance from the downsprue and strontium content. (a) 1 cm, 0.0004%; (b) 22.5 cm, 0.0004%; (c) 44 cm, 0.0004%; (d) 1 cm, 0.015%; (e) 22.5 cm, 0.015%; (f) 44 cm, 0.015%.

location in the casting, as shown in Fig. 9. At locations near the downsprue, the distribution is skewed towards large pores. Sections near the centre of the strip (22.5 cm), contain appreciable amounts of both small and large pores. The maximum pore density is observed at these locations as shown in Table VI. The maximum pore size decreases with distance from downsprue. For example, it can be seen from Table VI that the maximum pore size at distances of 1 and 44 cm from the downsprue are of the order of 380 000

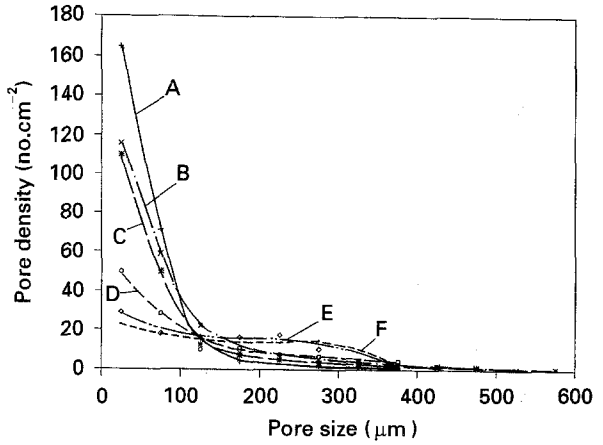

Figure 7 Pore distributions at a distance of 22.5 cm from the downsprue as a function of strontium content: (A) 0.0004%, (B) 0.0043%, (C) 0.0076%, (D) 0.0152%, (E) 0.0255%.

and 150 000 μm^2, respectively. In Fig. 9, curve C corresponds to a distance of 44 cm from downsprue or 1 cm behind the metal front. It should be noted that extensive amounts of porosity may be present in a zone very close to the metal front, i.e. a region about 7 mm behind the metal front (Fig. 10). Up to 6% porosity has been measured in this zone both for modified and unmodified alloys. The pores in this zone are essentially spherical as shown in Fig. 10. Further, surface porosity of up to 8% was detected in several castings as shown in Fig. 11. This surface porosity is observed for all strontium contents and is typically detected within about 5 mm from the free surface. Pores in this region are highly spherical (Fig. 11). Porosity data for modified sand and permanent mould castings are shown in Table VII. The maximum pore size and the amount of porosity are the lowest in permanent mould samples. The amount of porosity in EPC castings is comparable to the value measured in green sand castings.

Typical as-cast tensile properties measured in the test castings are shown in Table VIII. The properties of unmodified and modified alloys are identical. Strontium modification does not appear to have any beneficial effect on tensile strength or ductility. Tensile data for EPC castings are comparable to the measured values in sand castings. As can be expected, permanent mould castings have significantly higher values of UTS and elongation than sand or EPC samples.

4. Discussion

The addition of about 100 p.p.m. strontium to the melt produces a well-modified structure which has a rating of 4 or 5 on the AFS modification scale [16]. Additions of strontium in excess of 300 p.p.m. produces an overmodification effect. DasGupta *et al.* [17] have observed a similar coarsening effect in sand-cast A356 alloys. The reasons for the coarsening of silicon at high strontium contents are not clear, although recent results of Major and Rutter [18] can be used to explain some of the overmodification effects. The twin-plane reentrant edge (TPRE) model is perhaps the best available model for the growth of plate-like silicon. According to this model, growth of plate-like silicon in unmodified alloys occurs by repeated nucleation of new layers on the reentrant edges and grooves created by the intersection of {1 1 1} twins at the solidifying interface. When strontium is added to the melt, it may be preferentially absorbed at the silicon interface and lead to a poisoning effect, whereby the attachment of silicon on to the reentrant edges and grooves is prevented. Complete poisoning of the reentrant edges does not occur for strontium concentrations on the order of 0.03%. Major and Rutter suggest the following sequence of events during the growth of silicon in modified alloys: initial twin formation, TPRE growth for short distances until poisoning of the reentrant edges (after enough strontium is accumulated), and formation of new twins. This cycle repeats continuously and results in zig-zag growth of microfaceted silicon. At strontium concentrations greater than about 0.03%, the amount of strontium may be sufficient to suppress completely the TPRE growth. Under these conditions, the growth of silicon may be hindered until the undercooling at the interface has reached a sufficiently large value or until some of the strontium is consumed through the formation of strontium intermetallics. Such a mechanism may lead to the formation of an aluminum band, typical of an overmodified structure.

Several investigators have reported a reduction in mechanical properties beyond an optimum value of strontium. Closset and Gruzleski [19] report a reduction in tensile properties at strontium contents greater than 0.01%–0.015%. The data of Ozelton *et al.* [20] show that fracture properties of A356 alloys begin to decrease as the strontium concentration is increased beyond 0.01%–0.015%. This behaviour may originate from two distinct phenomena observed

TABLE IV Pore parameters at a distance of 22.5 cm from the downsprue as a function of strontium concentration

	Sr content (wt %)					
	0.0004	0.0043	0.0076	0.0108	0.0152	0.0255
Pore area (μm^2)						
Maximum	130000	210000	260000	180000	120000	110000
Average	4962	10795	11538	20872	21336	26911
Pore density (no. cm^{-2})	266	214	199	125	112	103
Aspect ratio	3.2	3.0	3.3	3.0	2.9	3.1
Porosity (%)	1.3	2.3	2.3	2.6	2.4	2.8

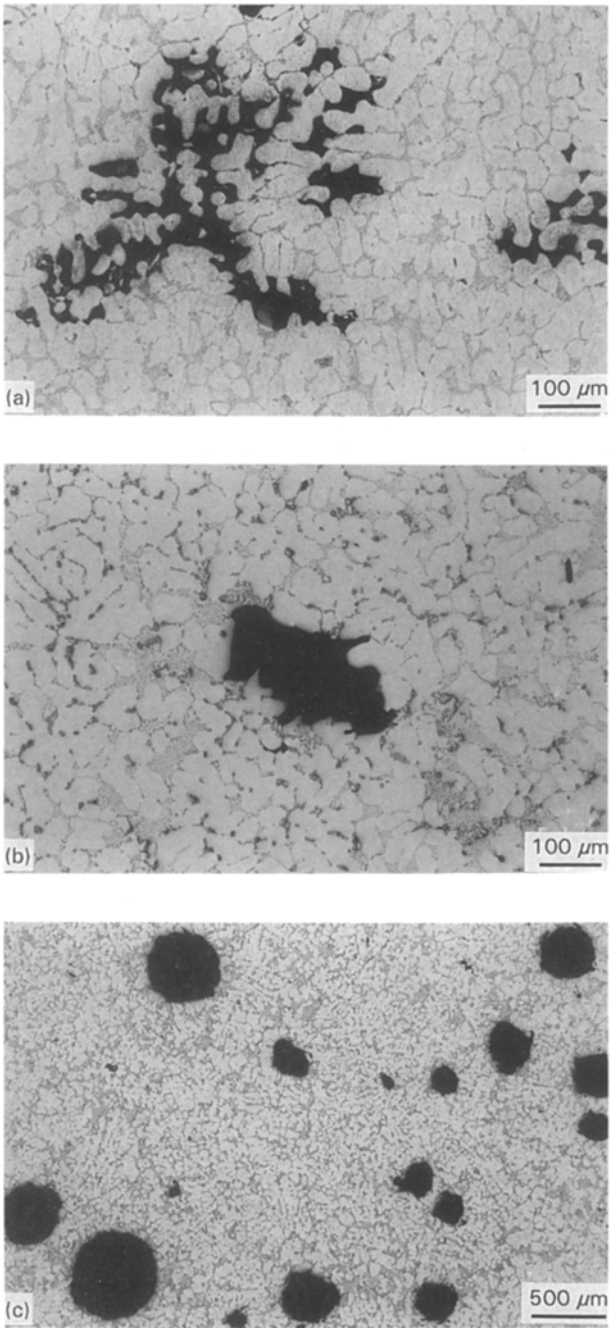

Figure 8 Classification of pores based on the circularity shape factor (CSF). (a) Highly irregular pores with CSF < 0.75; (b) intermediate pores with 0.75 < CSF < 0.85; (c) spherical pores with CSF > 0.85.

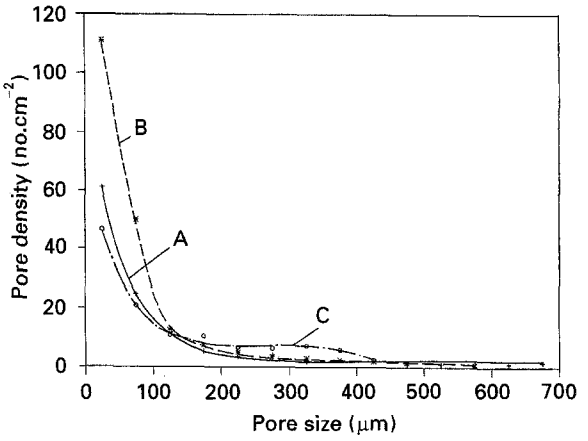

Figure 9 Pore distributions as a function of the distance from the downsprue for an alloy containing 0.0004% Sr. Distance from downsprue: (A) 1 cm, (B) 22.5 cm (C) 45 cm.

TABLE VI Variation of pore parameters with distance from downsprue in strontium modified (0.0076% Sr) castings

	Distance from downsprue		
	1 cm	22.5 cm	44 cm
Pore area (μm^2)			
Maximum	380000	260000	150000
Average	26159	11538	23990
Pore density (nc. cm^{-2})	122	199	117
Aspect ratio	2.97	3.27	3.04
Porosity (%)	3.2	2.3	2.8

in melts containing excessive amounts of strontium. As shown in Fig. 3, strontium concentrations greater than 0.015% result in the formation of coarse silicon particles. This coarsening may lead to a reduction in mechanical properties. In addition, at high strontium concentrations, angular intermetallics such as Al_4Sr and Al_4SrSi_2 particles may form, thereby lowering the mechanical properties [19]. Thus, optimum concentrations of strontium for both A356 and the 319 family of alloys are between 0.01% and 0.015%.

The physical mechanisms associated with the increase in the amount of porosity and in the maximum pore size upon strontium modification have not been clearly established. Some authors suggest that

TABLE V Distribution of pores based on the circularity shape factor (CSF) for the data shown in Table IV

	Sr content (wt %)					
	0.0004	0.0043	0.0076	0.0108	0.0152	0.0255
Classification based on number of pores						
CSF < 0.76	20.5%	16.7%	21.9%	17.8%	13.3%	13.0%
0.76 < CSF < 0.85	59.2%	50.9%	53.3%	46.2%	49.8%	50.6%
CSF > 0.85	20.3%	32.4%	24.8%	36.0%	36.9%	36.4%
Classification based on area						
CSF < 0.76	31.4%	32.6%	47.8%	20.6%	14.0%	13.5%
0.76 < CSF < 0.85	61.1%	48.0%	36.6%	44.4%	43.1%	40.9%
CSF > 0.85	7.5%	19.4%	15.6%	35.0%	42.9%	45.6%

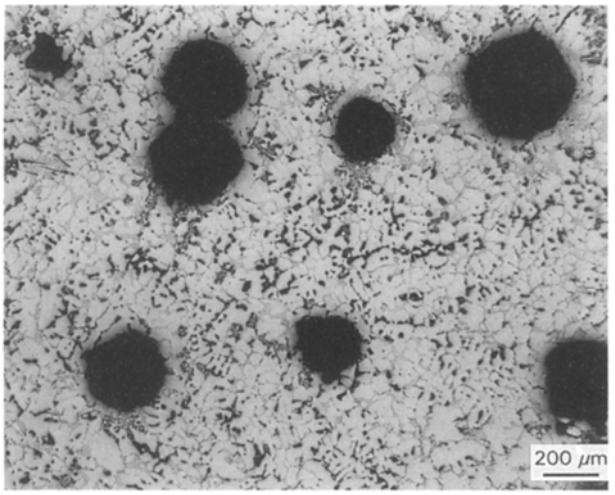

Figure 10 Photomicrograph showing extensive porosity in the casting at locations near the metal front. This porosity is typically observed within about 7 mm behind the metal front.

TABLE VII Pore parameters in modified (strontium concentration = 0.011%) EPC, green sand and permanent mould castings

	EPC	Green Sand	Permanent mould
Pore area (μm^2)			
Maximum	180000	190000	50000
Average	20872	12197	4674
Porosity (%)	2.6	3.2	0.7

TABLE VIII As-cast tensile properties in test castings

Condition	YS (MPa)	UTS (MPa)	Elongation (%)
EPC – unmodified	121	150	2.4
EPC – Sr modified	127	147	2.2
Green sand – modified	125	148	2.3
Permanent mould – modified	138	199	3.5

(Strontium level in modified castings = 0.01%)

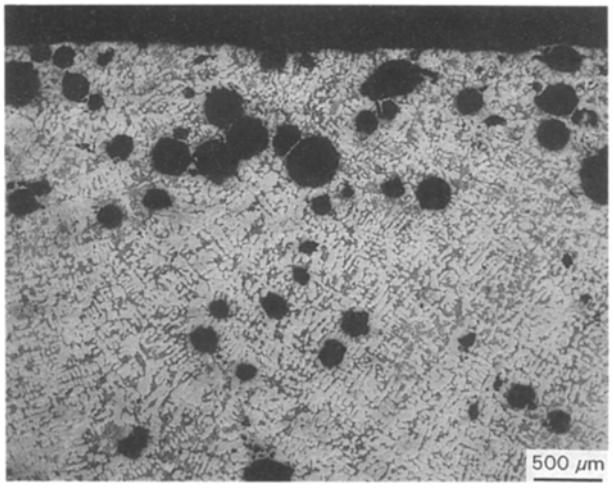

Figure 11 Photomicrograph showing surface porosity in EPC castings. This surface porosity is typically observed within about 5 mm below the free surface.

modification exacerbates porosity problems by increasing the hydrogen content of the melt and/or the rate of regassing of the melt [21, 22]. Others contend that the addition of strontium does not increase the hydrogen concentration or the rate of regassing [23, 24]. It is clear, however, that several factors may contribute to increased porosity in modified castings. The addition of reactive elements such as sodium and strontium to the melt may reduce the surface tension and may facilitate the nucleation of the pore. Recent data of Tynelius [25] and Fang and Granger [26] suggest that strontium may also increase the inclusion content of the melt and, thereby, provide additional sites for the nucleation of the pore. Oxide films and inclusions formed upon and addition of strontium may also provide boundaries along which the pores may expand, thereby increasing the maximum pore length in the solidified casting. In addition, it has been reported that modification increases the freezing range of the alloy [27]. Consequently, pores may form over a longer period and hence, may grow to large sizes. Argo and Gruzleski [28] indicate that large pores may be observed in modified alloys because of problems associated with interdendritic feeding. The reduction of eutectic temperature in modified alloys increases the length of the mushy zone and therefore large pockets of interdendritic liquid may become isolated. Solidification of this liquid may result in the formation of large pores. The morphology of the eutectic interface may also affect the distribution of microporosity. In unmodified alloys, the eutectic interface appears to be irregular, ragged and is not isothermal [25]. In this case, small localized regions of eutectic may grow ahead of the solidification front. Modified alloys, however, exhibit a macroscopically smooth, almost isothermal and distinctly scalloped interface. The extent of scalloping may be determined by the strontium content and on the local thermal conditions.

The pore distribution in cast aluminium alloys is strongly influenced by the solidification morphology. A356, a common foundry alloy, solidifies over a fairly narrow range ($\approx 60\,^{\circ}C$) and also contains relatively large amounts of eutectic liquid ($\approx 50\%$). Consequently, most of the pore growth occurs in the eutectic liquid and, hence, pores exhibit a high degree of circularity. Hence, in A356 alloys, about 50%–85% of the pores have a circularity shape factor greater than 0.85 [29]. Alloy 319, however, solidifies over a range of 105 °C and the fraction of eutectic is less than 30%. Because of the relatively large freezing range, interdendritic shrinkage may contribute significantly to the overall porosity. It is not surprising, therefore, that for moderate gas concentrations, the fraction of pores with CSF > 0.85 is between 7% and 45% (Table V).

The amount of bulk porosity and the pore characteristics of EPC castings are generally comparable to sand casting produced under similar gas and inclusion concentrations. EPC castings may, however, be prone to surface porosity (Fig. 11). The surface porosity may arise due to the presence of polymer liquid degradation products during solidification [10]. It has been

shown that the liquid residue that forms during the thermal degradation of the polymer may be absorbed by the coating. This liquid residue gradually depolymerizes completely to form the monomer gas, which may escape into the sand. Some of these gases may also diffuse back into the solidifying metal and may be entrapped as pores. The increase in porosity at the metal front (Fig. 10) may be caused by the entrapment of the gases resulting from the degradation of the polymer.

The tensile data shown in Table VIII do not show any significant difference between unmodified and modified alloys. Secondary alloys such as 319 may contain relatively large amounts of impurity elements which may form brittle compounds and hence, the tensile strength and ductility are not very sensitive to the morphology of interdendritic phases. However, recent results indicate that despite the increase in porosity, strontium modification can improve the impact and fracture properties substantially in heat-treated castings [30]. For example, it has been shown in 319-T6 castings the impact energy increases from 0.65 J to 2.0 J with the addition of 0.015% Strontium. In addition, heat-treatment times may be reduced substantially for strontium modified castings.

5. Conclusion

Strontium modification is becoming an increasingly common practice in aluminium foundries. The addition of about 0.01%–0.015% strontium produces a fibrous silicon structure. Strontium contents greater than about 0.015%–0.02% may lead to a coarsening of silicon particles and, consequently, are undesirable. This coarsening is consistent with the twin-plane re-entrant edge (TPRE) model for the growth of silicon. One of the major benefits of using strontium modification in alloys such as 319 is the refinement of iron- and copper-containing phases. The mechanical properties of the alloy are strongly influenced by the morphology of iron- and copper-rich phases and hence, any reduction in the size of these particles is highly desirable. The amount of bulk porosity and the pore characteristics of EPC castings are generally comparable to sand castings produced under similar gas and inclusion concentrations. EPC castings may, however, be prone to surface porosity. This surface porosity may arise due to the presence of polymer liquid degradation products during solidification. The addition of strontium leads to a significant change in pore characteristics. The number of highly irregular pores decreases and the fraction of nearly spherical pores increases. A large fraction of the porosity in modified alloys is present between the intergranular regions. In unmodified alloys, the large pores are along the grain boundaries, while many small pores are confined to the interdendritic regions. The amount of porosity and the pore size increase upon modification. The tensile properties of EPC castings are comparable to sand castings, but are lower than in permanent mould castings. Strontium modification does not appear to have an appreciable effect on tensile properties of 319 castings.

References

1. A. J. CLEGG, *Found. Trade J. Int.* **9** (1986) 51.
2. H. J. HEINE, *Found. M T* **114** (1986) 36.
3. G. del GAUDIO, G. SERRAMOGLIA, G. CAIRONI and G. TOSI, *Metall. Sci. Technol.* **3** (1985) 76.
4. A. J. CLEGG, *Found. Trade J.* **145** (1978) 393.
5. *Idem, ibid.*, **145** (1978) 149.
6. E. J. SIKORA, *Trans. AFS* **86** (1978) 65.
7. S. SHIVKUMAR and B. GALLOIS, *ibid.* **95** (1987) 791.
8. *Idem, ibid.* **95** (1987) 801.
9. S. SHIVKUMAR, L. WANG and B. STEENHOFF, *ibid.* **97** (1989) 825.
10. L. WANG, S. SHIVKUMAR and D. APELIAN, *ibid.* **98** (1990) 923.
11. S. SHIVKUMAR, L. WANG and D. APELIAN, *J. Metals* **42** (1990) 38.
12. G. SIGWORTH, *Trans. AFS* **91** (1983) 7.
13. G. SIGWORTH, S. SHIVKUMAR and D. APELIAN, *ibid.* **97** (1989) 811.
14. S. SHIVKUMAR, S. RICCI, B. STEENHOFF, D. APELIAN and G. SIGWORTH, *ibid.* **97** (1989) 791.
15. S. SHIVKUMAR, *ibid.* **101** (1993) 513–518.
16. G. SIGWORTH, *Mod. Casting* **77** (1987) 23.
17. R. DASGUPTA, C. G. BROWN and S. MAREK, *Trans. AFS* **96** (1988) 297.
18. J. F. MAJOR and J. W. RUTTER, *Mater. Sci. Technol.* **5** (1989) 645.
19. B. CLOSSET and J. E. GRUZLESKI, *Trans. AFS* **90** (1982) 453.
20. M. W. OZELTON, G. R. TURK and P. G. PORTER in "Proceedings of the Symposium on Technology for Premium Quality Castings", Denver, CO, February 1987, edited by E. Dunn and D. R. Durham (The Metallurgical Society, 1988) p. 81.
21. J. R. DENTON and J. A. SPITTLE, *Mater. Sci. Technol.* **1** (1985) 305.
22. J. CHARBONNIER, J. J. PERRIER and R. PORTALIER, *AFS Int. Cast Metals Res. J.* **3** (1978) 17.
23. F. DIMAYUGA, N. HANDIAK and J. E. GRUZLESKI, *Trans. AFS* **96** (1988) 83.
24. H. SHAHANI, *Scand. J. Metall.* **14** (1985) 306.
25. K. TYNELIUS, PhD thesis, Drexel University, Philadelphia, March 1992.
26. Q. T. FANG and D. A. GRANGER, *Trans. AFS* **97** (1989) 989.
27. M. D. HANNA, S. LU and A. HELLAWELL, *Metal. Trans.* **15A** (1984) 459.
28. D. ARGO and J. E. GRUZLESKI, *Trans. AFS* **96** (1988) 65.
29. S. SHIVKUMAR, L. WANG and R. LAVIGNE, in: "Proceedings of the Symposium on Light Metals", TMS Annual Meeting, Denver, Colorado, February 1993, edited by Subodh K. Das (The Metallurgical Society, 1993) p. 829.
30. S. SHIVKUMAR, L. WANG and C. KELLER, unpublished results (1993).

Received 6 May 1993
and accepted 5 August 1994